Letters in Applied NanoBioScience
Open-Access Journal (ISSN: 2284-6808)

Article
Volume 15, Issue 1, 2026, 49
https://doi.org/10.33263/LIANBS151.049

Synthesis, Spectral Analysis, Thermal Study, and in Vitro Antimicrobial Activity of Transition Metal Complexes of Schiff Base Derived from 4-Amino-1,2,4-Triazole-3-Thiol and 5-Bromosalicylaldehyde

Someshwar Bhale [1], Sunita Shinde [2], Sunil Tekale [3], Sandeep Dhotre [4], Rajendra Pawar [4,*]

[1] Department of Chemistry, Smt. G. G. Khadse College, Muktainagar, District Jalgaon (M.S.) 425306, India
[2] Department of Chemistry, MGM College of Engineering and Technology, Kamothe, Navi Mumbai (MS) 410209, India
[3] Department of Chemistry, Deogiri College, Aurangabad (MS) 431005, India
[4] Department of Chemistry, Shiv Chhatrapati College, Aurangabad (MS) 431003, India

Received: 27.04.2023; Accepted: 28.05.2024; Published: 30.03.2026

Abstract: A series of Co(II), Ni(II), Cu(II), and Zn(II) metal complexes have been prepared by using a molar ratio of ligand: metal as 1:1 with a newly synthesized Schiff base derived from 5-bromosalicylaldehyde and 4-amino-1,2,4-triazole-3-thiol by the condensation method. The structures of the Schiff base and its metal complexes were confirmed by IR, elemental analysis, 1H NMR, UV-Visible spectroscopy, TGA, and Mass spectrometry. The spectral data proved that the ligand acts as a binegative, tridentate. Based on spectral and analytical studies, an octahedral geometry has been assigned to Co(II) and Ni(II), whereas Cu(II) and Zn(II) are square planar and tetrahedral, respectively. The synthesized metal complexes, along with the ligand, were screened for antibacterial activity against bacterial species (*S. aureus*, *S. pyogenes*, *E. coli*, and *S. typhi*) and fungi (*C. albicans* and *T. rubrum*). The results of antimicrobial activity show that the metal complexes possessed better activity as compared to the Schiff base ligand.

Keywords: SNO donor ligand; metal complex; antimicrobial activity.

1. Introduction

The chemistry of 1,2,4-triazole and its derivatives is mostly remarkable because of the potential applications of these heterocyclic compounds in agricultural [1], medicinal [2], and other biodynamic activities [3-5]. Derivatives of 1,2,4-triazoles display a variety of biological activities such as antimicrobial [6], anticancer [7], anticonvulsant [8], anti-HIV [9], analgesic [10], and cytotoxic properties [11]. Besides, the 1,2,4-triazole nucleus constitutes a part of an extensive range of medicinally interesting molecules that act as better commercially marketed drugs such as Rizatriptan, Ribavirin, Alprazolam, and Fluconazole [12]. Therefore, there is a continuing motivation to explore these pharmacophores to improve novel molecules with diverse activities.

The transition metal complexes of 1,2,4-triazole-substituted moieties have been acknowledged as important due to their excellent coordination potential and diverse pharmacological properties [13]. Transition metals such as cobalt, nickel, copper, and zinc have a strong affinity for coordination due to their smaller size and higher nuclear charge [14]. Encouraged by these observations, it was contemplated to synthesize some new Schiff bases of 4-amino-1,2,4-triazole-3-thiol derivatives to explore their potency as better chemotherapeutic agents. The presence of a thiol group in the compound can bind to metal ions at the active site of the target. Thus, in the present article, we report the synthesis and characterization of transition metal(II)(Co(II), Ni(II), Cu(II), and Zn(II)) complexes with a tridentate ligand derived from the condensation of 5-bromosalicylaldehyde and 4-amino-1,2,4-triazole-3-thiol. The resulting metal(II) complexes were evaluated for their antifungal and antibacterial activity.

2. Materials and Methods

All the used chemicals were SD fine as well as Spectrochem-made and used without further purification. The 4-amino-1,2,4-triazole-3-thiol was synthesized according to the literature method. Melting points were determined on the PLT-276 digital melting point apparatus. Elemental analysis data were recorded using a Perkin-Elmer 240 elemental analyzer. IR spectra were scanned on a Bruker spectrometer in the range 4000-400 cm^{-1}. ^{1}H NMR and ^{13}C NMR spectra were recorded in DMSO-d$_6$ with Bruker Avance 200 MHz using TMS as the internal standard. UV absorption spectra and thermogravimetric analysis were recorded on Shimadzu UV-1800 and Shimadzu TGA 50 spectrometers, respectively.

2.1. Synthesis of 4-[(2-hydroxy-5-bromophenyl)methyleneimino]-3H-1,2,4-triazole-3-thiol (H2L).

The synthesis of 4-[(2-hydroxy-5-bromophenyl)methyleneimino]-3*H*-1,2,4-triazole-3-thiol was carried out according to the well-described procedure in the literature [15]. An equimolar quantity of 4-amino-1,2,4-triazole-3-thiol (0.580 g, 5 mmol) and 5-bromosalicyaldehyde (1.005 g, 5 mmol) were dissolved in 5 mL of acetic acid, and the resultant mixture was refluxed for 4 h under constant stirring.

Reaction progress was evaluated on TLC in (30% Ethyl acetate: n-hexane) as the mobile phase. After completion of the reaction, as confirmed by TCL, the reaction mixture was poured onto crushed ice and filtered off. The obtained product was recrystallized in absolute ethanol as a pure H_2L ligand (Scheme 1).

Color: Light yellow, Yield: 89 %, MP: 247 °C; FT-IR cm^{-1}: 3240 ν(-OH), 2530 ν(-SH), 1604 ν(C=N); ^{1}H NMR (200 MHz, DMSO-d$_6$): δ ppm 13.96 (s, 1H, thiol-SH), 10.87 (s, 1H, -OH), 9.73 (s, 1H, HC=N), 8.94 (s, 1H, triazole ring), 7.90 (d, *J* = 2.2 Hz, 1H, Ar-H), 7.60 (dd, *J* = 8.8, 2.3 Hz, 1H, Ar-H), 6.95 (d, *J* = 8.8 Hz, 1H, Ar-H); ^{13}C NMR (200 MHz, DMSO-*d*$_6$): δ ppm 162, 157, 155, 138, 136, 129, 120, 119, 110; Mass spectrum (ESI): *m/z:* 299 (found) $[H_2L]^+$.

2.2. General procedure for the synthesis of metal complexes (1-4).

Schiff base transition metal(II) complexes (1-4) of 4-[(2-hydroxy-5-bromophenyl)methyleneimino]-3H-1,2,4-triazole-3-thiol (H_2L) were synthesized from H_2L (0.29 g, 1 mmol) in methanol (20 mL) with corresponding metal(II) salts [i.e., chloride of Co(II) (0.24 g, 1 mmol), Ni(II) (0.24 g, 1 mmol), Cu(II) (0.17 g, 1 mmol) and Zn(II) (0.14 g, 1 mmol)] in methanol (10 mL) in 1:1 stoichiometry (Scheme 1). The pH of the solution was maintained slightly alkaline by adding aqueous ammonia. The solution was refluxed for 10-12 hrs. The solid product was separated under a vacuum and washed with cold methanol and diethyl ether (Yield: 65-81%).

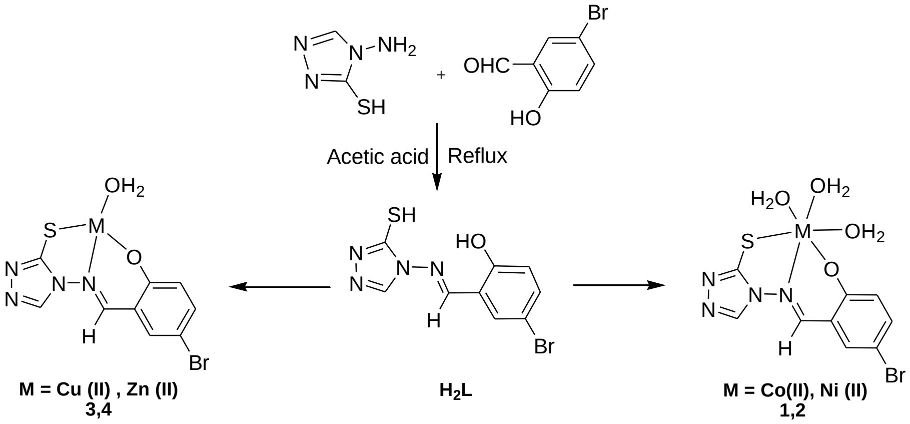

Scheme 1. Schematic route for the synthesis of H_2L ligand and its metal complexes.

3. Results and Discussion

All the prepared metal complexes were stable at room temperature, colored, non-hygroscopic, insoluble in water and many organic solvents, but soluble in DMF and DMSO. The elemental analysis data showed the formation of a 1:1 stoichiometry of the ML type. The physical and analytical data of the ligands and their metal complexes are shown in Table 1.

Table 1. Physical and analytical data of H_2L and its metal complexes.

Compound	**Mol. Formulae (F.W.)**	**M.P.°C**	**Color**	**Elemental analysis found (calculated.)%**			
				% C (cal.)	**% H (cal.)**	**% N (cal.)**	**% M (cal.)**
Ligand (H_2L)	$C_9H_7BrN_4OS$ (299.15)	247°C	Light Yellow	36.10 (36.13)	2.35 (2.36)	18.75 (18.73)	-
$[Co(L)(H_2O)_3]$	$C_9H_{11}BrCoN_4O_4S$ (410.11)	>280°C	Yellowish brown	26.10 (26.36)	2.60 (2.70)	13..70 (13.66)	14..25 (14.37)
$[Ni(L)(H_2O)_3]$	$C_9H_{11}BrN_4NiO_4S$ (409.87)	>280°C	Light green	26.40 (26.37)	2.62 (2.71)	13.52 (13.67)	14.50 (14.32)
$[Cu(L)(H_2O)_3]$	$C_9H_7BrCuN_4O_2S$ (378.79)	>280°C	Green	28.59 (28.54)	1.75 (1.86)	14.65 (14.79)	16.83 (16.78)
$[Zn(L)(H_2O)]$	$C_9H_7BrN_4O_2SZn$ (380.53)	>280°C	White	28.45 (28.41)	1.90 (1.85)	14.80 (14.72)	17.25 (17.18)

3.1. FT-IR spectra.

The characteristics of infrared bands of the Schiff base ligand and their corresponding metal complexes are listed in Table 2. The comparison of the IR spectra of the ligand and its metal complexes gives an idea about the potential binding sites of phenolic oxygen (-OH), azomethine nitrogen (-C=N), and thiol (-SH) that may participate in coordination with the metal ions. The positions of these peaks are expected to be altered upon complexation. It was observed that after chelation, ν(C=N) stretching vibration of the free ligand, which was at 1604 cm^{-1} shifted to lower wavenumbers in the metal complexes, indicating the involvement of the azomethine nitrogen in coordination [16]. The bands at 3241 and 2530 cm^{-1} in the IR spectrum of the free ligand, which correspond to the phenolic -OH and thiol -SH group, respectively, disappeared in metal complexes. This indicates the involvement of the deprotonated phenolic -OH and thiol -SH groups in chelation. Besides, new bands are found in the spectra of the metal complexes in the regions 555-540 cm^{-1} (phenolic-O), which are assigned to ν(M-O) stretching vibrations. The bands at 410-450 cm^{-1} in complexes have been assigned to ν(M-N) of the azomethine mode [15]. The bands for ν(M-S) stretching vibration could not be found because they would appear below 400 cm^{-1}. A lower frequency shift due to ν(C-S) in the IR spectra of metal complexes around 662-670 cm^{-1} further confirms this. The broadband in the region 3150-3390 cm^{-1} shows the presence of coordinated water molecules in the complexes. The same information is also supported by two bands in the range 789-830 cm^{-1} and 682-696 cm^{-1}, which correspond to rocking (H_2O) and wagging (H_2O) [16]. Hence, from the comparative study of IR spectra of ligands and complexes, it is concluded that ligand H_2L acts as a binegative, tridentate with ONS donor sites in complexes and coordinates to the metal ions through the azomethine-N and deprotonated phenolic-O and thiol -S.

Table 2. Characteristics IR bands and electronic transitions of the ligand and its metal complexes.

Compound	**ν(HC=N)**	**ν(-OH)**	**ν(-SH)**	**ν(M-N)**	**ν(M-O)**	**Electronic transition (cm^{-1})**
H_2L	1604	3240	2530	-	-	
$[Co(H_2L)(H_2O)_3]$	1602	-	-	423	543	10490,19810 (dd)
$[Ni (H_2L)(H_2O)_3]$	1596	-	-	433	542	11101,16399, 25499 (dd)
$[Cu (H_2L)(H_2O)]$	1598	-	-	465	520	19510 (dd)
$[Zn (H_2L) (H_2O)]$	1597	-	-	470	540	25000 (CT)

3.2 ^{1}H NMR spectra.

The ^{1}H NMR spectra of the ligand and Zn(II) complex were recorded in DMSO-d_6. The appearance of a characteristic singlet peak at δ 9.73 ppm confirms the formation of the Schiff-base ligand, which was assigned to the azomethine (CH=N) proton. A set of doublets and multiplets in the region 6.95-7.90 ppm was assigned to the aromatic protons, whereas a weak singlet at 13.96 ppm corresponds to -SH protons of the triazole ring. The proton of the -OH group appears as a singlet at 10.87 ppm.

In the ^{1}H NMR spectrum of the Zn(II) complex, a shift of electron density from ligand to metal ion has been observed. The imine proton signal was slightly deshielded, appearing at δ 9.12 ppm. This might be due to the donation of electron density from nitrogen to the zinc ion. Because of this electron transfer from nitrogen to zinc, a coordinate bond is formed between them (Zn⟵N) [16]. The characteristic signal for the -SH and -OH protons disappeared in the NMR of the zinc complex, which indicates the deprotonation of -SH and -OH protons during complexation. All other aromatic protons in the NMR spectrum of the zinc complex appeared at almost the same chemical shift as they appear in the spectrum of the ligand. The signal for coordinated water appeared as a broad singlet at δ 3.4 ppm.

3.3. Electronic spectra.

The electronic absorption spectra of all complexes were recorded in DMSO at room temperature, and the results are listed in Table 2. The electronic spectra of the cobalt complex show two transitions in the range of 10490 cm^{-1} and 19810 cm^{-1}, corresponding to ^4T1g (F)$\rightarrow ^4T_{2g}$(F) (ν_1); $^4T_{1g}$(F)$\rightarrow ^4T_{1g}$(P) (ν_3), ν_2 which is very close to (ν_3) transition is not observed, but it can be calculated [17] by using relation $\nu_2 = \nu_1 + 10Dq$. The position of these bands suggests an octahedral environment around the Co(II) ions. The electronic spectral data of the nickel complex displayed three d-d transitions in the region 11,101, 16,399, and 25,499 cm^{-1}, respectively, due to $^3A_{2g}(F) \rightarrow {}^3T_{2g}(F)$, $^3A_{2g}(F) \rightarrow {}^3T_{1g}(F)$ and $^3A_{2g}(F) \rightarrow {}^3T_{1g}(P)$ transitions. It strongly supports the octahedral geometry around Ni(II) ions.

In the case of the copper complex, the d-d transition was observed at 19,510 cm-1, which can be assigned as the $^2B_{1g} \rightarrow {}^2A_{1g}$ transition, indicating that the Cu(II) complex may exist in square planar geometry [18]. The moderately strong broadband for the zinc complex in the region 25000 cm^{-1} was assigned for the ligand-to-metal charge transfer transition (LMCT). The complex displays no appreciable absorptions in the region above 25000 cm^{-1} due to the d10 electronic configuration of the Zn(II) ion.

3.4. Thermal analysis.

The thermal behavior of the synthesized ligand and its metal complexes was studied by thermogravimetric analysis in a nitrogen atmosphere up to 800°C. The TGA curves were redrawn as % mass loss versus temperature. All metal complexes show the same decomposition pattern. The mass loss percentage, theoretical mass loss percentage, and the temperature range of several decomposition steps of all complexes are collectively given in Table 3, together with the evolved moiety. Thermal decomposition of the cobalt complex is completed in three steps within the temperature range 120-630°C. The first degradation step corresponds to eliminating three coordinated water molecules in the temperature range of 120-155°C. The second step corresponds to the removal of C_7H_4BrN in the temperature range of 155-370°C. In the third step, there was a loss of triazole moiety in the temperature range of 370-630°C, and as a final product, it leaves the metal oxide as a residue.

Table 3. Thermal analysis data of metal complexes (1-4).

Comp.no.	**Molecular formula**	**Stages**	**Temp (°C)**	**Possible evolved species**	**Residual species**	**Mass loss**	
						Found	**Calc.**
1	$C_9H_{11}BrCoN_4$ O_4S (410.11)	1st 2nd 3rd	120-155 155-370 370-630	$3H_2O$ C_7H_4BrN Triazole moiety	CoO	13.30 44.19 24.01 18.41	13.16 44.37 24.13 18.28
2	$C_9H_{11}BrN_4Ni$ O_4S (409.87)	1st 2nd 3rd	120-160 160-390 390-680	$3H_2O$ C_7H_4Br Triazole moiety	NiO	13.10 40.65 27.60 18.35	13.20 40.58 27.62 18.33
3	$C_9H_7BrCuN_4$ O_2S (378.79)	1st 2nd 3rd	135-165 165-420 420-660	H_2O C_7H_4BrN Triazole moiety	CuO	4.69 48.25 26.17 20.85	4.76 48.14 26.19 20.89
4	$C_9H_7BrN_4O_2$ SZn (380.53)	1st 2nd 3rd	130-163 163-358 358-695	H_2O C_7H_4BrN Triazole moiety	ZnO	4.75 47.92 26.10 21.18	4.73 47.89 26.05 21.31

3.5. Antimicrobial activity.

The antimicrobial activity of the synthesized compounds was carried out against four bacteria (*S. aureus, S. pyogenes, E. coli*, and *S. typhi*) and two fungi (*C. albicans & T. rubrum*) by a Petri-plate containing 30 mL PDA and nutrient agar medium. The plates were incubated for 20-24 hr and 24-48 hr for bacteria and fungi strains, respectively. The activities were measured in terms of the zone of inhibition in mm. Cefotaxime, Azithromycin, and Clotrimazole were used as the standard drugs for bacteria and fungi at a 500 ppm concentration of compounds and drugs.

The antimicrobial activity results are shown in Table 4. The metal complexes show higher inhibition against the tested microorganisms than the free ligand. The antimicrobial activity of metal complexes depends on the following factors: the chelate effect, the nature of the coordinated ligand, the total charge of the complex, the nature of the ion neutralizing the ionic complex, and the nuclearity of the metal center in the complex [19]. The increased activity of the metal complex compared to the free ligand can also be explained based on chelation theory [20].

Table 4. Antimicrobial activity data of synthesized compounds.

Compounds	**Diameter of Inhibition zone (mm)**					
	Antibacterial Activity				**Antifungal Activity**	
	S. Aureus	**S. Pyogenes**	**E. Coli**	**S. Typhi**	**C. Albicans**	**T. Rubrum**
Ligand (H_2L)	-	-	-	-	-	-
[$Co(H_2L)(H_2O)_3$]	-	-	07	09	-	-
[$Ni(H_2L)(H_2O)_3$]	-	-	-	-	-	-
[$Cu(H_2L)(H_2O)$]	20	18	-	05	03	-
[$Zn(H_2L)(H_2O)$]	08	-	-	06	-	-
Cefotaxime	-	-	**25**	**20**	-	-
Azithromycin	**26**	**24**	-	-	-	-
Clotrimazole	-	-	-	-	**18**	**25**

4. Conclusions

The synthesized ligand coordinates in a binegative tridentate manner around the metal(II) center in ML complexes. Based on spectral data, an octahedral geometry has been assigned for Co(II) and Ni(II) complexes, while the Cu(II) complex may exist in the square planar and tetrahedral forms for Zn(II) complexes. The ^{1}H NMR, IR, and TGA data confirmed the presence of coordinated water molecules. The antibacterial activity results show that all synthesized metal complexes exhibit moderate to significant inhibition against the tested strains. Based on activity data, the Cu(II) complex was found to be the most effective. All the metal complexes showed enhanced activity compared to the free ligand.

Author Contributions

Conceptualization, S. B. and R. P.; Methodology, S. B. and S. T.; Software, S. B.; Validation, S. B., S. S., and S. D.; Formal analysis, S. B., S. S., and S. D.; Investigation, S. B.; Resources, S. B. and R. P.; Data curation, S. S.; Writing – original draft, S. B.; Writing – review & editing, S. B. and R. P.; Visualization, S. B.; Supervision, R. P.; Project administration, S. B.; Funding acquisition, S. B. All authors have read and agreed to the published version of the manuscript.

Institutional Review Board Statement

Not applicable.

Informed Consent Statement

Not applicable.

Data Availability Statement

Data supporting the findings of this study are available upon reasonable request from the corresponding author.

Funding

This work received financial assistance under Senior Research Fellowship from the Council of Scientific and Industrial Research, New Delhi, India- File No. 22/12/2013(ii) EU-V

Acknowledgments

SPB is thankful to the Council of Scientific and Industrial Research for awarding a Senior Research Fellowship. We are thankful to the Principal of Deogiri College Aurangabad for providing the necessary laboratory facility and the Director, SAIF, Panjab University, Panjab, for providing spectral data.

Conflicts of Interest

The authors declare no conflict of interest.

Role of Funders

The Council of Scientific and Industrial Research awarded a Senior Research Fellowship to Someshwar Bhale.

Abbreviations

The following abbreviations are used in this manuscript:

^{13}C NMR	Carbon-13 Nuclear Magnetic Resonance
DMF	N,N-Dimethyl Formamide
DMSO	Dimethyl Sulfoxide
DMSO-d_6	Deuterated Dimethyl Sulfoxide
ESI	Electron Spray Ionization
FT- IR	Fourier transform infrared spectroscopy
HIV	Human immunodeficiency virus
^{1}H NMR	Proton Nuclear Magnetic Resonance
mL	milliliter
Mmol	Millimole
MP	Melting Point
TGA	Thermogravimetric Analysis
TLC	Thin Layer Chromatography
TMS	Tetramethylsilane
UV	Ultra Violet

References

1. Shao, W.B.; Wang, P.Y.; Fang, Z.M.; Wang, J.J.; Guo, D.X.; Ji, J.; Zhou, X.; Qi, P.Y.; Liu, L.W.; Yang, S. Synthesis and biological evaluation of 1, 2, 4-triazole thioethers as both potential virulence factor inhibitors against plant bacterial diseases and agricultural antiviral agents against tobacco mosaic virus infections. *J. Agri. & Food Chem.* **2021**, *69*,15108-15122, https://doi.org/10.1021/acs.jafc.1c05202.

2. Sameliuk, Y.; Kaplaushenko, T.; Al Zedan, F. 1, 2, 4-Triazole derivatives in medicine and pharmacy and application prospects. *J. Facul. Pharm. Ankara Univ.* **2021**, *45*, 598-614, https://doi.org/10.33483/jfpau.885888.
3. Li, J.; Zhang, J. The antibacterial activity of 1, 2, 3-triazole-and 1, 2, 4-triazole-containing hybrids against Staphylococcus aureus: An updated review (2020-present). *Curr. Top. Med. Chem.* **2022**, *22*, 41-63, https://doi.org/10.2174/1568026621666211111160332.
4. Mohamed, A.M.; El-Sayed, W.A.; Ibrahim, A.A.; Abdel-Hafez, N.A.; Ali, K.A.; Mohamed, S.F. Recent trends in the chemistry of [1, 2, 4] Triazole [1, 5-a] pyrimidines. *Org. Prep. Proced. Int.* **2021**, *53*, 211-239, https://doi.org/10.1080/00304948.2020.1871310
5. Kumari, M.; Tahlan, S.; Narasimhan, B.; Ramasamy, K.; Lim, S.M.; Shah, S.A.A.; Mani, V.; Kakkar, S.; Synthesis and biological evaluation of heterocyclic 1, 2, 4-triazole scaffolds as promising pharmacological agents. *BMC Chem.* **2021**, *15*, 1-16, https://doi.org/10.1186/s13065-020-00717-y.
6. Gomha, S.M.; Edrees, M.M.; Muhammad, Z.A.; Kheder, N.A.; Abu-Melha, S.; Saad, A.M. Synthesis, characterization, and antimicrobial evaluation of some new 1, 4-dihydropyridines-1, 2, 4-triazole hybrid compounds. *Poly. Arom. Comp.* **2021**, *42*, 173-185, https://doi.org/10.1080/10406638.2020.1720751.
7. Turky, A.; Bayoumi, A.H.; Sherbiny, F.F.; El-Adl, K.; Abulkhair, H.S.. Unravelling the anticancer potency of 1, 2, 4-triazole-N-arylamide hybrids through inhibition of STAT3: Synthesis and in silico mechanistic studies. *Mol. Div.* **2021**, *25*, 403-420, https://doi.org/10.1007/s11030-020-10131-0.
8. Wang, Y.; Liu, D. An Important potential anti-epileptic/anticonvulsant active group: A review of 1, 2, 4-triazole groups and their action. *Drug Res.* **2022**, *72*, 131-138, https://doi.org/10.1055/a-1670-6992.
9. Jiang, X.; Sharma, P.P.; Rathi, B.; Ji, X.; Hu, L.; Gao, Z.; Kang, D.; Wang, Z.; Xie, M.; Xu, S.; Zhang, X. Discovery of novel 1, 2, 4-triazole phenylalanine derivatives targeting an unexplored region within the interprotomer pocket of the HIV capsid protein. *J. Med. Virol.* **2022**, *94*, 5975-5986, https://doi.org/10.1002/jmv.28064.
10. Salgın-Gökşen, U.; Gökhan-Kelekçi, N.; Göktaş, Ö.; Köysal, Y.; Kılıç, E.; Işık, Ş.; Aktay, G.; Özalp, M. 1-Acylthiosemicarbazides, 1, 2, 4-triazole-5 (4H)-thiones. 1, 3, 4-thiadiazoles and hydrazones containing 5-methyl-2-benzoxazolinones: Synthesis, analgesic-anti-inflammatory and antimicrobial activities. *Bioorg. Med. Chem.* **2007**, *15*, 5738-5751, https://doi.org/10.1016/j.bmc.2007.06.006.
11. Shahid, W.; Ashraf, M.; Saleem, M.; Bashir, B.; Muzaffar, S.; Ali, M.; Kaleem, A.; Amjad, H.; Bhattarai, K.; Riaz, N.; Exploring phenylcarbamoylazinane-1, 2, 4-triazole thioethers as lipoxygenase inhibitors supported with in vitro, in silico and cytotoxic studies. *Bioorg. Chem.* **2021**, *115*, 105261, https://doi.org/10.1016/j.bioorg.2021.105261.
12. Sumrra, S.H.; Zafar, W.; Imran, M.; Chohan, Z.H. A review on the biomedical efficacy of transition metal triazole compounds. *J. Coord. Chem.* **2022**, *75*, 293-334, https://doi.org/10.1080/00958972.2022.2059359.
13. Mahmoud, N.F.; Abbas, A.A.; Mohamed, G.G. Synthesis, characterization, antimicrobial, and MOE evaluation of nano 1, 2, 4-triazole-based Schiff base ligand with some d-block metal ions. *Appl. Organomet. Chem.* **2021**, *35*, e6219, https://doi.org/10.1002/aoc.6219.
14. Yadav, S., Yashas, S.R. and Shivaraju, H.P. Transitional metal chalcogenide nanostructures for remediation and energy: A review. *Env. Chem. Lett.* **2021**, *19*, 3683-3700, https://doi.org/10.1007/s10311-021-01269-w.
15. Bhale, S.P.; Tekale, S.U.; Yadav, A.R.; Pathare, P.G. ; Franguelli, F. P.; Kótai, L.; Pawar, R.P. Synthesis, characterization and antimicrobial activity of transition metal complexes of 4-[(2- hydroxy-4-methoxyphenyl)methyleneamino]-2,4- dihydro-3H-1,2,4-triazole-3-thione. *Eur. Chem. Bull.*, **2020**, *9*, 430-435, http://dx.doi.org/10.17628/ecb.2020.9.430-435.
16. Deswal, Y.; Asija, S.; Kumar, D.; Jindal, D.K.; Chandan, G.; Panwar, V.; Saroya, S.; Kumar, N. Transition metal complexes of triazole-based bioactive ligands: Synthesis, spectral characterization, antimicrobial, anticancer and molecular docking studies. *Res. Chem. Int.* **2022**, *48*, 703-729, https://doi.org/10.1007/s11164-021-04621-5.
17. Yadav, M.; Sharma, S.; Devi, J. Designing, spectroscopic characterization, biological screening and antioxidant activity of mononuclear transition metal complexes of bidentate Schiff base hydrazones. *J. Chem. Sci.* **2021**, *133*, 1-22, https://doi.org/10.1007/s12039-020-01854-6.
18. Fathima, S.S.A.; Meeran, M.M.S.; Nagarajan, E.R. Synthesis, characterization and biological evaluation of novel 2,2′-((1,2-diphenylethane-1,2-diylidene)bis(azanylylidene))bis(pyridin-3-ol)and metal complexes: Molecular docking and in silico ADMET profile. *Stru. Chem.* **2019**, *31*, 521-539, https://doi.org/10.1007/s11224-019-01425-7.

19. El-Gammal, O.A.; Mohamed, F.S.; Rezk, G.N.; El-Bindary, A.A. Structural characterization and biological activity of a new metal complexes based of Schiff base. *J. Mol. Liq.* **2021**, *330*, 115522, https://doi.org/10.1016/j.molliq.2021.115522.
20. Kotian, A.; Kumara, K.; Kamat, V.; Naik, K.; Kokare, D.G.; Nevrekar, A.; Lokanath, N.K.; Revankar, V.K. p-halo N4-phenyl substituted thiosemicarbazones: Crystal structure, supramolecular architecture, characterization and bio-assay of their Co(III) and Ni(II) complexes. *J. Mol. Struct*. **2018**, *1156*, 115-126, https://doi.org/10.1016/j.molstruc.2017.11.098.

Publisher’s Note & Disclaimer